Modeled and observed empirical orthogonal functions of currents in the Yucatan Channel, Gulf of Mexico

Lie-Yauw Oey and Tal Ezer

Program in Atmospheric and Oceanic Sciences, Princeton University, Princeton, New Jersey, USA

Wilton Sturges

Department of Oceanography, Florida State University, Tallahassee, Florida, USA

[1] *Candela et al.* [2003] have reported empirical orthogonal function (EOF) analyses based on 23-month current-meter and acoustic Doppler current profiler measurements in the Yucatan Channel. Those authors noted the difference between EOFs obtained from observations and their *z*-level models and EOFs calculated by *Ezer et al.* [2003] from the results of a terrain-following model. Here a new analysis is reported that explains this difference, and that also suggests the importance of shelf-edge meander mode of the core Loop Current in the channel. We show that the terrain-following model gives EOFs with characteristics similar to those observed when data from the upper slope and shelf in the western portion of the model channel are omitted. Modes 1 and 2 have tripole and dipole structures with energies (35%, 26%), respectively, of total energy, and correlate with "slow" vacillation of the core-current for periods >50 days. Exclusion of upper-slope and shelf data eliminates a short-period and energetic component inherent in Ezer et al.'s original mode 1 EOF. This mode correlates with frontal meanders of the core current over the shelf edge in the western portion of the channel. The short-period mode may be missing or underestimated in observational and *z*-level models' analyses, since there were only a few moorings over the upper slope and shelf, and *z*-level models have step-like topography with generally lower resolution in shallower seas.   INDEX TERMS: 4576 Oceanography: Physical: Western boundary currents; 4219 Oceanography: General: Continental shelf processes; 4255 Oceanography: General: Numerical modeling; KEYWORDS: Yucatan Channel, EOFs, frontal meanders

1. Introduction

[2] *Candela et al.* [2003] [also *Abascal et al.*, 2003] have reported analyses based on a remarkable data set they have obtained in the Yucatan Channel. The observations consist of, among other things, 23-month current-meter and acoustic Doppler current profiler (ADCP) measurements across the channel. On the basis of these data the authors computed empirical orthogonal functions (EOFs) of currents in the channel. The EOF mode 1 (referred to as OEOF1 for observed EOF mode 1) accounts for about 31% of the total energy and shows a tripolar structure primarily restricted in the upper $z > -500$ m of water, where z is positive upward and $z = 0$ is the mean sea surface. Thus OEOF1 has coherent currents on both sides and opposing currents in the center of the channel (Figure 1, bottom). Mode 2 (i.e., OEOF2) accounts for about 23% of the total energy and exhibits a bipolar structure that extends deeper to $z \approx -1000$ m. *Candela*

et al. [2003] also reported EOFs from two grid configurations of the Océan Parallélisé (OPA) *z*-level primitive equation model: one at 1/6° resolution and the other one at finer 1/12° resolution. To force their models, they used daily surface fluxes from the European Centre for Medium-Range Weather Forecasts (ECMWF): 1979–1983 for the 1/6° resolution, and 1999–2001 for the 1/12° resolution. Both models give a bipolar mode 1 with about 60% of the total energy, and a tripolar mode 2 with about 20% of the total energy. The modeled and observed EOFs are generally similar, though details differ (e.g., the order of modes is switched, or periods are longer in models ≈100 days compared to ≈20–100 days in observations [*Abascal et al.*, 2003], and also the western core of the modeled tripolar structure is subsurface, etc).

[3] In a separate study, *Ezer et al.* [2003] computed EOFs based on the results of a terrain-following model of the Gulf of Mexico and Yucatan Channel (the Princeton Ocean Model (POM) [*Oey et al.*, 2003]. The model is forced by 6-hourly ECMWF wind from 1993 through 1996. The resulting modes 1 and 2 (referred to as EEOF1 and EEOF2 for Ezer et al.'s EOF modes 1 and 2,
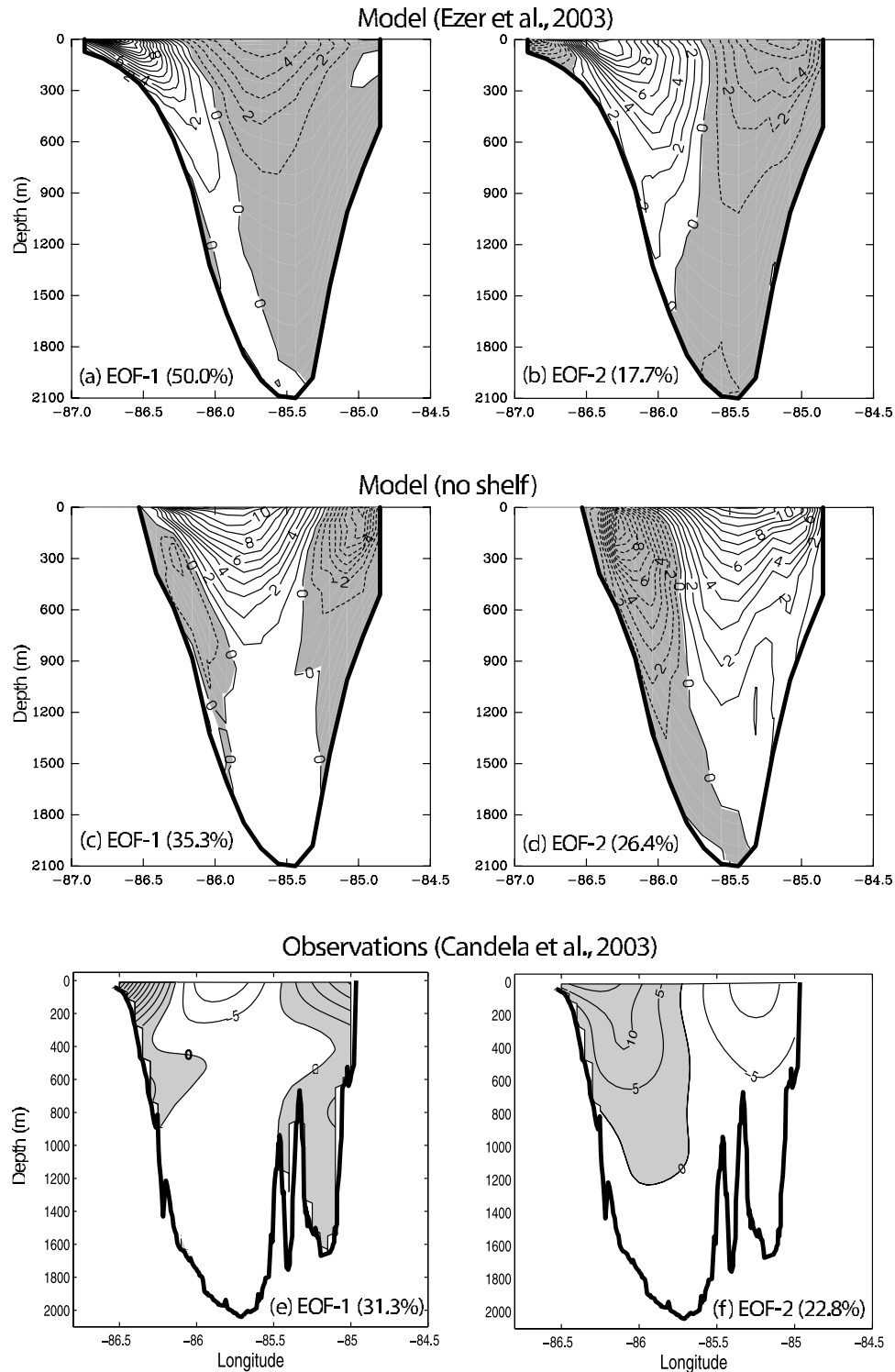
Figure 1. Empirical orthogonal function modes 1 and 2 for (top) terrain-following model results of *Ezer et al.* [2003], (middle) same model but with data from the upper slope and shelf on the western side of the channel omitted, and (bottom) observations of *Candela et al.* [2003]. Contour intervals are 1/100 of normalized amplitude for models and cm s^{-1} for observation.

respectively) are shown in Figure 1 (top). EEOF1 contains 50% of the total energy, and *Ezer et al.* [2003] show that this mode closely correlates with cross-channel meander of the near-surface core current in the channel (the correlation coefficient $\gamma = 0.83$). EEOF2 contains

18% of the energy and correlates with inflow transport fluctuations ($\gamma = 0.7$; note this is not total transport, but rather is that part of the transport that is northward (i.e., "inflow") into the Gulf). *Candela et al.* [2003] note that EEOF1 (Figure 1a) is different from OEOF1 (Figure 1e).
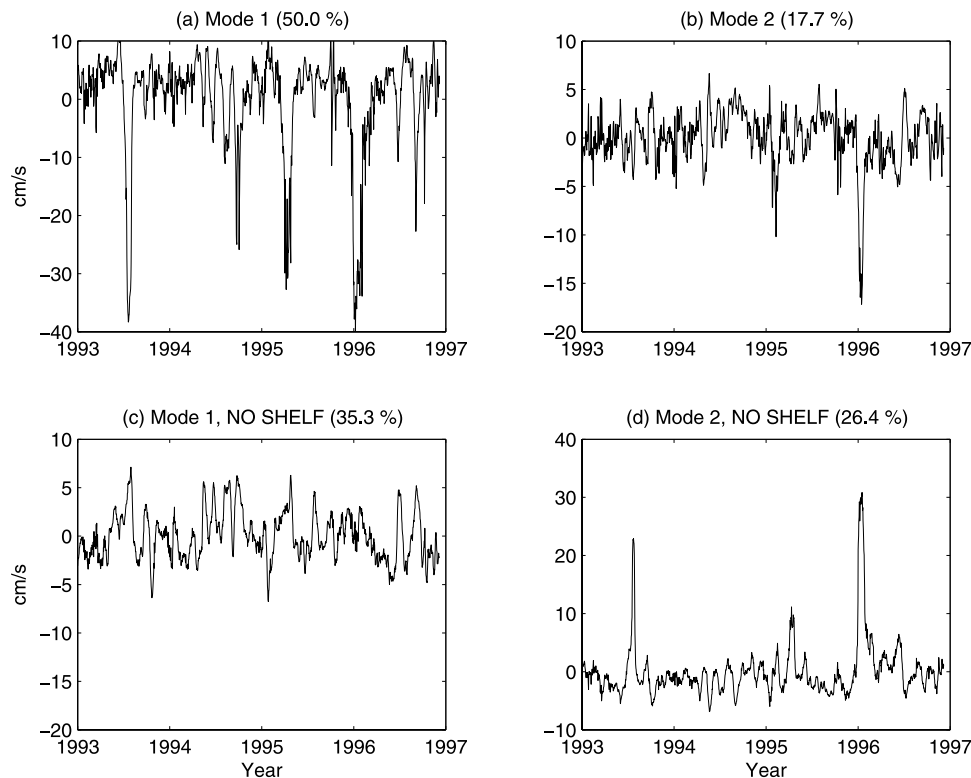
Figure 2. Time series of the empirical orthogonal function modes (left) 1 and (right) 2. Top row is for *Ezer et al.*'s [2003] terrain-following model results, while bottom row is for the same model but with data from the upper slope and shelf on the western side of the channel omitted.

Below, we offer a plausible explanation for this apparent discrepancy.

2. Explaining the Discrepancy

[4] The existence of the meander mode 1 (EEOF1) in *Ezer et al.*'s [2003] analysis depends on cross-channel vacillations of the core Loop Current in the Yucatan Channel. As is well known, observations of many types have shown that a western boundary current along a shelf-break is characterized by meanders especially in the near-surface layers ($\approx$upper 300 m) west of the maximum current core (i.e., the cyclonic side [e.g., *Lee and Atkinson*, 1983; *Sugimoto et al.*, 1988]). Typical meander periods are <30 days and length scales are $50 \sim 150$ km. Near-surface waters of the core current can intrude shoreward or "spill" onto the outer shelf [*Atkinson et al.*, 1989]. A terrain-following grid uses its full number of vertical grid cells (we use 24) to model these meander and intrusion processes. In other words, our model "sees" a leaky shelfbreak. For comparison, the z-level OPA model has $13 \sim 14$ cells in water depth of 300 m, and $8 \sim 9$ cells in 100 m.

[5] A comparison of the topographies in *Candela et al.*'s [2003] observations and z-level models with the topography incorporated in *Ezer et al.*'s [2003] terrain-following model (compare top and bottom rows of Figure 1) suggests that the meander mode may be underestimated by Candela et al. The westernmost observation mooring is located just east of 86.5°W, and there are two moorings west of the maximum current core [see *Candela et al.*, 2003, Figures 1 and 2]. It is

possible therefore that the EOF analysis can miss a good portion of flow variability over the upper slope and shelf (water depths shallower than about 300 m) on the western side of the channel. The same may be said of the z-level models. The step-like representation of topography and lack of vertical resolution in shallow seas in z-level models do not in general accurately simulate slope and shelf processes [e.g., *Killworth et al.*, 1991; *Gerdes*, 1993].

[6] To test the above idea, we repeated *Ezer et al.*'s [2003] analysis but artificially omitted modeled currents over the western slope and shelf of the channel (i.e., west of 86.5°W). The resulting modes 1 and 2 (referred to as NEOF1 and NEOF2, respectively, for "no-shelf" EOFs) are shown in Figure 1 (middle row). NEOF1 now shows a tripolar structure similar to OEOF1, and NEOF2 shows a deeper bipolar structure similar to OEOF2. Not only is the observed mode order retained, but the mode 1 and 2 energy partition (35%, 26%) is also close to the observed partition (31%, 23%). Figure 2 gives the corresponding EOF time series and shows that the omission of upper slope and shelf removes higher-frequency fluctuations (periods less than about 30 days), and relegates the original mode 1 (i.e., EEOF1; Figure 2a) to the new mode 2 (i.e., NEOF2; Figure 2d) with reduced amplitude. The original mode 2 (i.e., EEOF2; Figure 2b) now becomes new mode 1 (i.e., NEOF1; Figure 2c), also with smaller amplitudes. While the switching of modes (i.e., EEOF1 → NEOF2 and EEOF2 → NEOF1) cannot be exact; Figure 2 indicates that the absence of a "leaky" upper slope and shelf all but eliminates the energetic high-frequency meander mode

Table 1. Modeled EOF and Meander Correlations[a]

Frequency Band, days	With Upper Slope and Shelf		Without Upper Slope and Shelf	
	EEOF 1 (50%)	EEOF 2 (18%)	NEOF 1 (35%)	NEOF 2 (26%)
<50	0.70	–	0.75	–
>50	0.85	–	0.64	0.76

[a]Dashes indicate insignificant values at the 95% confidence level. Changes from modes with upper slope and shelf to those without are EEOF1 → NEOF2 and EEOF2 → NEOF1.

(compare Figure 2a with Figure 2d, and Figure 2b with Figure 2c). Spectrum analysis (not shown) indicates that most of the energy of the new modes is in the 40 ∼ 100 days band, somewhat redder than the observed band especially for mode 2 (20 ∼ 100 days [*Abascal et al.*, 2003]). As with the z-level models, some other details also differ; for example, the western core of the modeled tripolar structure is subsurface.

3. Discussion

[7] The difference between the EOFs calculated by *Candela et al.* [2003] [also *Abascal et al.*, 2003] and *Ezer et al.* [2003] can therefore be attributed to an additional mode that existed in the latter authors' analysis. Below, we give supporting evidence that this mode is related to generally shorter-period meanderings of the core current over the upper slope and shelf in the western portion of the Yucatan Channel.

[8] *Abascal et al.* [2003] interpreted both OEOF1 and OEOF2 in terms of passages of eddies (anticyclones and cyclones) or anomalies, through the channel (see their Figure 18). These anomalies give rise to meanders of the core current. We may generalize their ideas by categorizing the core-current meander into energies contained primarily in processes due to (1) small-scale, short-period frontal meanders [*Lee and Atkinson*, 1983; *Sugimoto et al.*, 1988] and (2) large-amplitude vacillation caused by dynamics related to eddy shedding [e.g., *Ezer et al.*, 2003] and/or by eddies propagating through the channel [*Abascal et al.*, 2003]. The latter authors show that OEOF1 relates to meanders and has energy predominantly at longer periods, 50 ∼ 100 days (see their Figures 11 and 13). Although not explicitly mentioned by these authors, OEOF2 also appears to visually relate to meanders (compare their Figures 10d and 11a) and contains energies in both the 50 ∼ 100 day and 20 ∼ 40 day bands. As mentioned above, Ezer et al. found good correlation between EEOF1 and meanders, but EEOF2 was found to correlate instead with inflow transport. To understand how Ezer et al.'s findings relate to the EOFs found here without the upper slope and shelf (i.e., to NEOF1 and 2), and also to Abascal et al.'s results, we conduct cross-correlation analyses of the models' EOFs (both with and without the upper slope and shelf) with the core-current positions (i.e., with meanders) in the channel. Table 1 summarizes the results in terms of correlations in two bands: periods of <50 days and >50 days.

3.1. EEOF1 and NEOF2

[9] The EEOF1 is seen to correlate well with meanders in both bands, while the correlation between EEOF2 and meanders is insignificant (and poor). Now, EEOF1 becomes NEOF2 when the upper slope and shelf are excluded, and

Table 1 indicates that NEOF2 correlates with meanders at the longer-period band >50 days. This result is consistent with Figure 2, mentioned previously, which shows that short-period fluctuations are eliminated when upper slope and shelf are excluded. In fact, we find that as much as 70% of the energy in EEOF1 is eliminated when the upper slope and shelf are excluded. Therefore most of the energy in EEOF1 actually resides in shorter-period frontal meanders over the upper slope and shelf (i.e., process 1 above). The remaining, longer-period fluctuations relate to the slower cross-channel vacillation of the core current (i.e., process 2).

3.2. EEOF2 and NEOF1

[10] Table 1 indicates that while EEOF2 does not correlate with current meander, its counterpart without the upper slope and shelf, NEOF1, now correlates with meanders in both bands. This result (i.e., that NEOF1 correlates with meanders) agrees with *Abascal et al.* [2003], who found that the observed mode 1 (OEOF1) also correlates with meanders. The reduction of energy from EEOF2 to NEOF1 is now only 27%, and we find that, as with EEOF2, NEOF1 correlates with inflow transport, though γ is lower = 0.48 (the significance level = 0.4) instead of γ = 0.7 for EEOF2 [*Ezer et al.*, 2003]. Since inflow transport depends on current variability over the entire channel, rather than specifically on processes over the western slope and shelf, we may conclude that NEOF1 contains more energy that relates to the slower cross-channel vacillation of the core current (i.e., again, process 2). The spectrum of NEOF1 (not shown) confirms this inference, as it indicates a prominent peak at 80 ∼ 120 days, with successively smaller peaks around 40 days and 20 days. This result also agrees with *Abascal et al.* [2003], who note that the spectrum of OEOF1 is skewed toward longer periods of 50 ∼ 100 days. The similarities between NEOF1 and OEOF1 (i.e., they both are skewed toward longer periods and both relate to meanders) and the fact that NEOF1 is a degenerate form of EEOF2 strongly suggest that OEOF1, too, may be a degenerate form of a mode that would account more completely for variability over the upper slope and shelf: an observed mode that is a counterpart of Ezer et al.'s mode 2 EOF (i.e., of EEOF2).

[11] In summary, the above considerations suggest that *Ezer et al.*'s [2003] EOF modes (1 and 2) are reversed analogues of the observed modes. EEOF1 is analogous to OEOF2, but disguised by the dominance of short-period frontal meander variability over the upper slope and shelf in the western portion of the current core. Similarly, EEOF2 is analogous to OEOF1, except that its western portion of the tripolar structure resides over the upper slope and shelf (compare Figures 1b and 1e). Once the upper slope and shelf are eliminated, this western structure becomes con-

centrated subsurface (Figure 1c). (Note that the western structure of OEOF1 (Figure 1e) appears to also have a subsurface maximum, though it is weak in comparison to surface values.) The z-level OPA models also show a subsurface variance concentration rather than the observed surface concentration of variance.

[12] The reversals of modes in *Ezer et al.*'s [2003] model modes when compared with the observed modes may also be applicable to the z-level models. The z-level models have energy partition: (tripolar, bipolar) = (20%, 60%), compared to (31%, 23%) for observations and (35%, 26%) for our model without the upper slope and shelf. It would be interesting to check if the comparison with observations might be "improved" if the upper slope and shelf of the z-level model are also omitted.

3.3. Two Additional Checks

[13] First, we make sure that our model's high vertical resolution near the surface, with grid spacing $\Delta z \approx 5$ m, does not bias the EOFs. We repeated the analyses with a subsampled grid, so that $\Delta z \approx 45$ m near the surface. The resulting EOFs are virtually identical. Second, local (along slope) winds can produce cross-slope motions [e.g., *Atkinson et al.*, 1989]. To be more precise, then, the preceding discussions may be generalized by lumping wind-induced processes with fluctuations caused by short-period shelf-edge meanders, and the conclusions would not change. We have, however, also computed the importance of wind. We find little correlations between currents (and meanders) and the local ECMWF winds used in the model. The local prevailing winds are cross channel and are inefficient in driving the predominantly along-slope currents [e.g., *Csanady*, 1982]. These findings are consistent with those of *Abascal et al.* [2003], who found little correlations between transport fluctuations with local winds, and also with those of *Oey et al.* [2003], who found strong channel responses only by remote wind stress curl in the central Caribbean Sea and the Atlantic. On the other hand, along-channel, Ekman currents are produced in the model in the synoptic weather band $5 \sim 10$ days, but these exist throughout the channel in the surface layer ($\sim$50 m), are weak ($\sim$0.05 m s^{-1}), and furthermore weaken on both sides of the channel. Thus Ekman fluctuations are not only weak, but they also affect the analyses both with and without the upper slope and shelf. Therefore we can interpret differences between the EOFs with and without the upper slope and shelf primarily in terms of short-period shelf-edge meanders.

4. Conclusion

[14] Our results suggest that shelf-edge meanders of the core current play a key role in a more complete description of the current variability in the Yucatan Channel. While we have proposed above that meanders in the channel may be categorized into short-period shelf-edge processes and slow cross-channel vacillation of the core current, we are reluctant to be specific about the nature of these fluctuations (for example, whether they are due to passing eddies, Loop Current dynamics, frontal instabilities, or even are wind induced, etc.). The proposed short-period shelf-edge physics that govern the interaction between currents over the shelf/slope and in the main channel remain to be further studied with observations that resolve the upper slope and shelf. A detailed comparison of the model with such observations would also address one reviewer's concern if the model with a shelf may overestimate the high-frequency variations.

References

Abascal, A. J., J. Sheinbaum, J. Candela, J. Ochoa, and A. Badan (2003), Analysis of flow variability in the Yucatan Channel, *J. Geophys. Res.*, *108*(C12), 3381, doi:10.1029/2003JC001922.

Atkinson, L. P., E. Oka, S. Y. Wu, T. J. Berger, J. O. Blanton, and T. N. Lee (1989), Hydrographic variability of southeastern U.S. shelf and slope waters during the Genesis of Atlantic Lows Experiment: Winter 1986, *J. Geophys. Res.*, *94*, 10,699–10,713.

Candela, J., S. Tanahara, M. Crepon, B. Barnier, and J. Sheinbaum (2003), Yucatan Channel flow: Observations versus CLIPPER ATL6 and MERCATOR PAM models, *J. Geophys. Res.*, *108*(C12), 3385, doi:10.1029/2003JC001961.

Csanady, G. T. (1982), *Circulation in the Coastal Ocean*, 279 pp., Reidel, Norwell, Mass.

Ezer, T., L.-Y. Oey, W. Sturges, and H.-C. Lee (2003), The variability of currents in the Yucatan Channel: Analysis of results from a numerical ocean model, *J. Geophys. Res.*, *108*(C1), 3012, doi:10.1029/2002JC001509.

Gerdes, R. (1993), A primitive equation ocean circulation model using a general vertical coordinate transformation: 1. Description and testing of the model, *J. Geophys. Res.*, *98*, 14,683–14,701.

Killworth, P. D., D. Stainforth, D. J. Webb, and S. M. Paterson (1991), The development of a free-surface Bryan-Cox-Semtner ocean model, *J. Phys. Oceanogr.*, *21*, 1333–1348.

Lee, T. N., and L. P. Atkinson (1983), Low-frequency current and temperature variability from Gulf Stream frontal eddies and atmospheric forcing along the southeast U.S. outer continental shelf, *J. Geophys. Res.*, *88*, 4541–4567.

Oey, L.-Y., H.-C. Lee, and W. J. Schmitz Jr. (2003), Effects of winds and Caribbean eddies on the frequency of loop current eddy shedding: A numerical model study, *J. Geophys. Res.*, *108*(C10), 3324, doi:10.1029/2002JC001698.

Sugimoto, T., S. Kimura, and K. Miyaji (1988), Meander of the Kuroshio front and current variability in the East China Sea, *J. Oceanogr. Soc. Jpn.*, *44*, 125–135.

————————

T. Ezer and L.-Y. Oey, Program in Atmospheric and Oceanic Sciences, Princeton University, Sayre Hall, Forestal Campus, Princeton, NJ 08544, USA. (ezer@splash.princeton.edu; lyo@princeton.edu)

W. Sturges, Department of Oceanography, Florida State University, Tallahassee, FL 32306, USA. (sturges@ocean.fsu.edu)